



Influence of Lower Tropospheric Moisture on Local Soil Moisture-Precipitation Feedback over the U.S. Southern Great Plains

5 Gaoyun Wang^{1,2,3}, Rong Fu², Yizhou Zhuang², Paul A. Dirmeyer⁴, Joseph A. Santanello⁵, Guiling Wang⁶, Kun Yang⁷, Kaighin McColl⁸

¹Department of Atmospheric and Oceanic Sciences, School of Physics, Peking University, Beijing, China

²Department of Atmospheric and Oceanic Sciences, University of California, Los Angeles, CA, USA

³The High School Affiliated to Southern University of Science and Technology, Shenzhen, China

10 ⁴Department of Atmospheric, Oceanic and Earth Sciences, George Mason University, Fairfax, VA, USA

⁵NASA Godard Space Flight Center, Greenbelt, MD, USA

⁶Department of Civil and Environmental Engineering, University of Connecticut, Storrs, CT, USA

⁷Department of Earth System Science, Tsinghua University, Beijing, China

⁸Department of Earth and Planetary Sciences, Harvard University, Cambridge, MA, USA

Correspondence to: Yizhou Zhuang (zhuangyz@atmos.ucla.edu)

15

Abstract. Land-atmosphere coupling (LAC) has long been studied focusing on land surface and atmospheric boundary layer processes. However, the influence of lower tropospheric (LT) humidity on LAC remains largely unexplored. In this study, we use radiosonde observations from the U.S. Southern Great Plains (SGP) site and an entrained parcel buoyancy model to investigate the impact of LT humidity on LAC there during the warm season (May-September). We quantify the effect of LT humidity on convective buoyancy by measuring the difference between the 2-4 km vertically integrated buoyancy with and without the influence of background LT humidity. Our results show that, under dry soil conditions, anomalously high LT humidity is necessary to produce the buoyancy profiles required for afternoon precipitation events (APEs). These APEs under dry soil moisture cannot be explained by commonly used local land-atmosphere coupling indices such as the convective triggering potential/low-level humidity index (CTP/HI_{Low}), which do not account for the influence of the LT humidity. On the other hand, consideration of LT humidity is unnecessary to explain APEs under wet soil moisture conditions, suggesting the boundary layer moisture alone could be sufficient to generate the required buoyancy profiles. These findings highlight the need to consider the impact of LT humidity, which is often decoupled from the humidity near the surface and largely controlled by moisture transport, in understanding land-atmospheric feedbacks over dry soil conditions, especially during droughts or dry spells over the SGP.

20
25
30

1 Introduction

Land-atmosphere coupling (LAC) plays an important role in determining local and regional climate variability, including surface temperature, humidity, cloud, precipitation, and climate extremes such as drought and floods, especially during the warm season over interior continents (e.g. Fernando et al., 2016; Koster et al., 2004, 2006; Guo et al., 2006; Wang et al., 2007; Roundy and Santanello, 2017; Santanello et al., 2009; Konings et al., 2010; Song et

35



al., 2016; Roundy et al., 2013). To provide a consistent characterization of land-atmosphere coupling, the International Global Energy and Water Exchanges Project (GEWEX) developed the Local Land-Atmosphere Coupling (LoCo) initiative to coordinate and promote process-level metrics that quantify and characterize LAC (Santanello et al., 2018). The LoCo initiative develops a suite of integrative metrics to quantify the complex relationships and feedback between
40 the land surface and atmosphere. For example, the mixing diagram approach (Santanello et al., 2009) relates the daytime coevolution of 2-m potential temperature and humidity to the energy and water budgets and growth of the planetary boundary layer (PBL). The convective triggering potential/low-level humidity index (CTP/ HL_{Low} ; Findell & Eltahir, 2003) characterizes the lower tropospheric lapse rate and dewpoint depression of the PBL for convection. The heated condensation framework (HCF, Tawfik et al., 2015a, 2015b) diagnoses the contribution of surface fluxes
45 to convective initiation based on temperature and humidity profiles. The soil moisture-precipitation (SM-P) feedback is one of the most extensively studied land-atmospheric feedbacks in the literature (e.g. Koster et al., 2004; Ferguson & Wood, 2010; Roundy & Santanello, 2017; Santanello et al., 2018), particularly regarding its effects on the frequency and intensity of convective precipitation (e.g. Taylor, 2015; Tuttle & Salvucci, 2016; Yin et al., 2015).
LoCo investigates the links in the chain coupling soil moisture with the PBL, which connect through surface fluxes,
50 2-meter temperature and humidity, PBL growth and entrainment, cloud, and precipitation. However, the humidity in the lower troposphere (LT) above the PBL is not explicitly included in previous research. Recent research indicates that specific humidity in the LT (q_{LT}) plays a central role in triggering (or the development of) deep convection in the tropics, subtropics, and mid-latitudes during the warm season (Bretherton et al., 2004; Holloway and Neelin, 2009; Zhang and Klein, 2010; Zhuang et al., 2018) and in the convective initiation driven by land surface heating (Tawfik
55 et al., 2015b, a). The lateral entrainment of q_{LT} dominates buoyancy above the PBL, which is crucial for deep convection development, while entrainment of air at the cloud base has a stronger influence on shallow convection (Holloway and Neelin, 2009; Mapes et al., 2006).
A moist LT can enhance convection by entraining moist air plumes, while low LT humidity can dilute moist plumes originating from the PBL, thereby interfering with the surface influence on convection and precipitation. Thus, q_{LT}
60 determines whether shallow convection can develop into deep convection locally (Schiro et al., 2016; Zhang and Klein, 2010; Zhuang et al., 2017, 2018) and the occurrence and intensity of mesoscale convection (Schiro et al., 2018). q_{LT} is influenced by moisture transport from the PBL (which is largely influenced by land surface), horizontal moisture advection, and subsidence that mixes dry air from aloft. Therefore, it is important to study the relative influences of
land surface versus large-scale atmospheric circulation on rainfall and clouds. In this study, we explore the effect of
65 LT humidity on the SM-P relationship to determine whether it can significantly influence the local LAC. The dataset and methods are described in section 2. The results are reported in section 3. Discussion and conclusions are provided in section 4.



2 Data and method

2.1 Dataset

70 This study focuses on the local warm season (May-September) when thermodynamically driven convection is most prevalent and land-surface feedback plays an important role in determining precipitation (Myoung and Nielsen-Gammon, 2010). Unless stated otherwise, all measurements are taken at the U.S. Department of Energy's Atmospheric Radiation Measurement (DOE ARM) Southern Great Plain (SGP) central facility (CF) and the region within a 50-km radius of the CF for the period of 2001-2019. Below are the specific details about the datasets used in this study.

75 2.1.1 Sounding Profiles

Sounding profile data at the SGP CF were obtained through balloon sonde observation. Data immediately before noon, specifically at 11:30 local standard time (LST) were used in this study as they best represent the preconditions of afternoon convection. Because the vertical levels vary with each sounding, data were re-gridded into a uniform vertical resolution of 20 m to facilitate composite analysis. Profiles of the dry-bulb temperature (T), dew point temperature (T_d), and atmospheric pressure (p) were used to calculate the mixing ratio (r), specific humidity (q), and buoyancy (b) using the entrained parcel model (described in section 2.2.1). The data used are available online at <https://www.arm.gov/capabilities/instruments/sonde>.

2.1.2 Soil moisture

Fractional water index (FWI) is a normalized measurement specifically developed for the Campbell 229-L soil moisture sensor and ranges from 0 for very dry soil to 1 for saturated soil (Schneider et al., 2003). FWI can capture soil wetness independent of soil texture, so it standardizes the observation and allows for intercomparison among different sites with different soil types. Most root biomass in the SGP region and its vicinity is within the top 30 cm of the soil profile (e.g., Raz-Yaseef et al., 2015). Because evapotranspiration, a vital link in the SM-P relationship, is heavily influenced by plant and root zone soil moisture, we used FWI at 25 cm measurement depth from a surface station near the SGP CF. The 30-min-averaged Oklahoma Mesonet Soil Moisture (OKMSOIL) value-added product (VAP) was used to represent soil wetness (available at <https://www.arm.gov/capabilities/vaps/okmsoil>). Wet soils are defined as those with FWI greater than 0.7, which is considered optimal for the plant, and dry soils are defined as FWI smaller than 0.4, which could result in water stress and plant wilting (Illston et al., 2008; Wakefield et al., 2019).

2.1.3 Precipitation

95 We utilize hourly gridded precipitation products from Arkansas-Red Basin River Forecast Center (ABRFC) based on WSR-88D Nexrad radar precipitation estimates combined with rain gauge reports with extensive quality control (Fulton et al., 1998). The data is available online at <https://www.arm.gov/capabilities/vaps/abrfc>. We used spatially averaged data over the region within a 50 km radius of the SGP CF for this study.



2.1.4 PBL height

100 We applied the boundary layer regime identified by the criteria defined in Liu and Liang (2010) to estimate the PBL height by using gradients of potential temperature profiles from the sounding observations that are available four times per day. This data is available at <https://www.arm.gov/capabilities/vaps/pblht>.

2.2 Quantifying contributions of surface and LT humidity to convective buoyancy

105 Previous research on local land-atmosphere interaction mainly focused on the influence of surface flux and moisture in the PBL on convection initiation and precipitation, such as those related to HCF and mixing diagram metrics. The CTP/ HI_{Low} metric considers the effect of lapse rate 100-300 hPa (or about 2-4 km) above ground level (AGL) on vertically integrated buoyancy in the LT (i.e., CTP) and humidity of the PBL (i.e., HI_{Low}), but it does not account for the impact of LT moisture.

110 Isolating the local influence from other factors in observation is challenging. In this study, we use the correlation between specific humidity (q) in the LT and that at the near-surface layer to infer the potential influence of the land surface on the LT moisture (Figure 1). As expected, the correlation between the q near the surface and that in the PBL is significant and larger than 0.95. Above the PBL, the correlation between q of LT and q in the near-surface layer decreases rapidly with height. The LT humidity is still significantly correlated to near-surface moisture above 2km, which indicates the potential influence from the surface. To separate the effect of the land surface, we define a coupled
115 LT humidity profile from 2 km to 4 km AGL related to the land surface moisture condition, which is reconstructed from the linear regression between q profile of this layer and the averaged q within the mixed layer.

To quantify the direct influence of LT moisture on convective buoyancy, we adopt an entraining parcel model used in Zhuang et al. (2018). In this model, the air parcel is lifted with the initial condition of average value within the mixed layer. The ascending air parcel then goes through three processes at each vertical level: dry adiabatic process (parcel
120 ascends without interacting with the environment, entropy conservation), entrainment process (interacts with ambient air, enthalpy conservation), precipitation process (releases condensate, temperature conservation). We apply the deep inflow-A entrainment (DIA) scheme which has been shown to more realistically represent the buoyancy profile required for deep convection compared to the other assumptions of the lateral entrainment rates such as the constant fractional entrainment rate scheme (e.g., Holloway & Neelin, 2009; Schiro et al., 2016; Siebesma et al., 2007). The
125 DIA scheme uses an entrainment rate inversely proportional to the altitude (αz^{-1}) for simplicity. All condensates formed from the previous two processes are set to fall out in the precipitation process (pseudo-adiabatic process). And finally, buoyancy is calculated by $b = g \frac{T_{pv} - T_{ev}}{T_{ev}}$, where T_{pv} and T_{ev} are the virtual temperature of the parcel and the environment, respectively. Details of this model are provided in Zhuang et al. (2018).

To quantify the influence of LT humidity on the lateral entrainment of the convection and, consequently, the buoyancy
130 of the convective air parcel, we consider two q profiles for the lateral entrainment process: 1) the observed humidity profile (q_R) and 2) the land-coupled humidity profile (q_{LC}). The q_{LC} below 2 km AGL equals to the observed q , and q_{LC} between 2 km and 4 km AGL is a coupled LT humidity profile constructed from the regression between q and averaged q in the mixed layer (as described in 2.2). Since the effect of entrainment accumulates continuously after the parcel is lifted, we calculate the buoyancy profile with q_R as humidity profile (b_R) and that with q_{LC} as humidity



135 profile (b_{LC}), and then use the vertical integral of their difference in the LT (2-4 km AGL), $B_{LT} = \int_{2 \text{ km AGL}}^{4 \text{ km AGL}} (b_R - b_{LC}) dz$, to quantify the additional effect of LT moisture variation on the parcel buoyancy that is not coupled with the PBL. We also calculate the integral of buoyancy based on q_{LC} , i.e., $B_{LC} = \int_{2 \text{ km AGL}}^{4 \text{ km AGL}} b_{LC} dz$, to assess the land-coupled effect on convection. To make the results comparable, we apply a normal percentile transform (Wilks, 2011) to obtain standardized scores of B_{LT} , which we use for further analysis.

140 2.3 Identify dry/wet soil regime and coupled afternoon precipitation events

The CTP/HI_{Low} framework developed by Findell & Eltahir (2003) is commonly used to identify atmospheric preference of LAC state. CTP is calculated by integrating the difference between moist adiabat temperature and the ambient temperature profile from 100 to 300 hPa AGL. It is a measure of the energy available for convection and the 100–300 hPa AGL is a critical level for the development of the daytime boundary layer. HI_{Low}, on the other hand, indicates the pre-existing moisture of the very lower atmosphere, and is defined as HI_{Low} = $(T - T_d)_{150 \text{ hPa AGL}} + (T - T_d)_{50 \text{ hPa AGL}}$. In this framework, wet soil advantage regime occurs when the atmospheric state is closer to the wet adiabatic rate, resulting in a low CTP and triggering convection through a strong increase in moist static energy from the land surface moisture (small HI_{Low}). Conversely, dry soil advantage regime occurs when the temperature profile is close to the dry adiabatic lapse rate with weak thermal stability (high CTP), and the soil provides less water vapor but more heat. This condition favors convection lifted by the boundary layer growth due to high sensible heat fluxes at the surface (Ek and Holtslag, 2004; Huang and Margulis, 2011; Gentine et al., 2013).

We adopt a modified CTP/HI_{Low} framework proposed by Wakefield et al. (2019) using the standardized score of CTP/HI_{Low}. As in Wakefield et al. (2019), dry-coupling cases are defined by anomalously high CTP (higher than climatological CTP for our analysis period) over dry soils (FWI < 0.4), which is similar to the dry soil advantage regime in Findell & Eltahir (2003). Wet-coupling cases, on the other hand, are characterized by anomalously low HI_{Low} over wet soil (FWI > 0.7), which corresponds to a moisture-abundant, energy-limited regime where the atmospheric profile is likely near moist adiabatic (Findell and Eltahir, 2003). The wet soil condition is expected to promote precipitation recycling through the addition of moist static energy via evapotranspiration and provides a continuous supply of low-level moisture.

160 Since LAC would mostly affect the thermodynamically driven afternoon convection, we focus on the morning (0600-1300 LST), afternoon (1400-2000 LST), and evening (2100-2400 LST) precipitation events in our analysis. Afternoon precipitation events (APEs) are identified as daily samples that meet the following two criteria: 1) daily precipitation peaks during the afternoon hours defined above; and 2) the afternoon precipitation is at least twice as large as the morning precipitation, and also greater than the evening precipitation (filter out organized precipitation). The cases not categorized as APEs are referred to as non-APEs afterward. We obtain a total of 368 APEs from the 2172 sounding. We further select APEs associated with either dry-coupling or wet-coupling condition, resulting in 94 dry-coupling APEs and 79 wet-coupling APEs, which account for 24.2% of the total 388 dry-coupling cases and 20.3 % of the total 389 wet-coupling cases, respectively.



3 Results

170 3.1 Thermodynamic pre-conditions for APEs under the dry and wet-coupling regimes

To identify favorable atmospheric conditions for coupling APEs, we evaluate the differences in temperature (T), specific humidity (q), and relative humidity (RH) at 11:30 LST between averaged local coupling APEs and non-APE cases in the warm seasons (May to September), as shown in Figure 2. Regardless of soil moisture conditions and coupling regimes, APEs are always associated with a wetter lower troposphere (0-4 km) than non-APEs. For dry-coupling regimes, the increases of q and RH in the PBL and the LT associated with APEs are also stronger than those with the non-APEs, especially between 0.5 km and 3.5 km AGL, and the contrast between APEs and non-APEs in dry-coupling regime is larger than that for wet-coupling regimes. These humidity differences are expected, as more humid pre-conditions favor the occurrence of APEs. Notice that the greatest contrast between RH of APEs and that of non-APEs occurs between 1 km and 3.5 km AGL (above the PBL), which is the combined result of high q and decreasing T over this layer, highlighting the possible strong influence of LT humidity on deep convection.

In contrast, the sign of the temperature difference between APEs and non-APEs below 1.7 km AGL varies between the dry-coupling and wet-coupling regimes. For the dry-coupling regimes, the average temperature of APEs is lower than that of the non-APEs. This is presumably due to the stronger surface sensible flux and less stable atmosphere (a steep lapse rate or faster decrease of temperature with height) associated with APEs than the non-APEs under the dry-coupling regime. For the wet-coupling regime, the average temperature of the APEs is warmer than that of the non-APEs below 1.7 km AGL. This is consistent with a weaker lapse rate associated with a more humid environment, presumably due to vertical mixing of shallow convection, in the APEs than in the non-APEs cases. Above 1.7 km AGL, temperature of the APEs cases is lower than that of the non-APEs for both dry and wet-coupling regimes, as expected from less stable thermodynamic conditions in the APEs than in the non-APEs.

To investigate the difference in atmospheric conditions that favor APEs under the dry- versus wet-coupling regime, we compare the composite differential profiles of RH, q , and T between dry- and wet-coupling APEs, as shown in Figure 3. In general, T is higher for APEs under dry-coupling than under wet-coupling regime (Figure 3a), especially in the PBL (below 2 km). This can be attributed to stronger sensible heat flux and temperature mixing over a dry surface. Notably, there is a significant difference in LT specific humidity between dry- and wet-coupling regimes (Figure 3b), with q associated with APEs being slightly lower below 1 km AGL under dry-coupling than under wet-coupling regime, but higher above 1 km, especially between 2 km and 3 km AGL. This suggests that APEs require entrainment of higher LT moisture under dry-coupling than under wet-coupling regimes. Both Figures 2b and 3b suggest that higher LT specific humidity is needed for APEs under the dry-coupling than under the wet-coupling regimes. Moreover, RH associated with dry-coupling regimes is less than that of wet-coupling regimes in the PBL (Figure 3c), as expected from a drier PBL over a dry surface. However, such an RH difference becomes smaller and eventually disappears in the LT (2-4 km). This is because the lower RH in the dry-coupling regimes is mainly due to warmer T below 2 km AGL (Figure 3b), whereas above 2 km AGL, the higher q and slightly warmer T in the dry-coupling regimes balance each other out and lead to a similar RH as in the wet-coupling regimes.

Recent studies on the SM-P relationship have highlighted the greater impact of soil-moisture anomalies on boundary-layer stability and precipitation formation than on the ambient moisture (e.g., Seneviratne et al., 2010; Santanello et



al., 2018). To investigate how humidity affects the preconditioning of the convective environment and how it impacts instability in dry- and wet-coupling regimes, we use an entraining parcel model to calculate buoyancy profiles for b_R and b_{LC} , respectively, with parcels originating in the mixed layer. We then compute differences in the integral buoyancy between b_R and b_{LC} profiles for the 2-4 km AGL range to explore the influence of LT humidity-related convective thermodynamic instability.

To evaluate the atmospheric thermodynamic structure associated with the B_{LT} , we evaluate the composite average sounding profiles based on three tertiles of B_{LT} in the warm season as shown in Figure 4. The B_{LT} values for the three tertiles range from -55.8 to -8.8 J/kg, -8.8 to 10.20 J/kg, and 10.0 to 72.8 J/kg, respectively. It is noteworthy that the temperature and dew point are similar among these three tertiles of B_{LT} near the surface (below 900 hPa) but clearly different from above 900 hPa up to at least 400 hPa AGL, which indicates the importance of LT humidity.

For the lower tertile (0% - 33%) of B_{LT} (Figure 4a), dew point values are substantially lower than those for the middle and upper tertile of the B_{LT} (Figures 4b and 4c). The sharp decrease of dew point values with height, near-constant temperature, and large gap between the temperature and dew point profiles at 700-900 hPa suggest strong dry shallow convection. For the middle tertile (Figure 4b), dewpoint and temperature decrease gradually with a height between 900 hPa and 700 hPa, and the gap between the dew point and temperature profiles is smaller than those for the lower tertile of the B_{LT} (Figure 4a). These features suggest a mixture of dry and moist shallow convection. For the upper tertile of B_{LT} (Figure 4c, 67% - 100%), dew point values are nearly constant from the surface to 700 hPa, and the humidity of free troposphere, as indicated by the gap between temperature and dew point profiles, is substantially wetter (implying higher RH) than for the middle and lower tertile of the B_{LT} . These features suggest that moist shallow convection dominates LT. Higher dew point values between 700 hPa and 500 hPa also suggest a more humid middle troposphere associated with the upper B_{LT} tertile (Figure 4c) than with the middle and lower B_{LT} tertile (Figure 4a and 4b). Thus, Figure 4 suggests that B_{LT} variations are strongly influenced by the humidity in the lower and middle troposphere.

3.2 The influence of LT humidity on afternoon precipitation under different LAC regimes

To investigate the effect of the LT humidity versus land surface air humidity on APEs, we evaluate the probability distribution of APEs as a function of B_{LT} and B_{LC} for dry- and wet-coupling APEs, respectively, in Figure 5. B_{LC} is usually more negative over dry soil (Figure 5b) than over wet soil (Figure 5a), and therefore usually more negative over dry PBL than over wet PBL. Figure 5b shows that dry-coupling APEs occur more frequently with negative B_{LC} (69%) and positive B_{LT} (77%), indicating that the influence of a more humid LT can override the influence of surface air aridity. For land surface, favoring local precipitation ($B_{LC} > 0$), dry-coupling APEs occur more frequently with positive B_{LT} (26%) than with negative B_{LT} (5%). For the wet-coupling conditions, 57% of APEs occur with positive B_{LT} , while 31% occur with humid PBL pre-condition (Figure 5a). Overall, for dry-coupling cases, more APEs are associated with humid LT (positive B_{LT}) than with humid surface air (positive B_{LC}), but this trend is not evident for wet-coupling cases.

To evaluate the influence of LT humidity on LAC under the CTP/HI_{Low} framework, we compare the joint distribution of all APEs, wet-coupling APEs, and dry-coupling APEs, respectively, as a function of B_{LT} scores and HI_{Low} scores



(Figure S1) using a normal percentile transform (Wilks 2011). Larger than normal B_{LT} (humid LT) values were associated with 61% of all APEs, regardless of the PBL humidity. Smaller than normal HI_{Low} (humid PBL) occurred in 63% of all APEs, regardless of the LT humidity. About 40% of all APEs occur under both humid PBL and humid
245 LT. Thus, the probabilities for APEs to occur under either humid PBL or humid LT are similar, with a preference for APEs to occur under both humid PBL and humid LT conditions. For dry-coupling condition, 76% of the APEs occur under humid LT versus 59% under humid PBL. Therefore, APEs appear to prefer humid LT more than humid PBL under dry-coupling conditions, but this preference is not found in wet-coupling conditions. This result is consistent with the findings in Figure 5.

250 To further investigate how LT humidity or B_{LT} can affect the probability of APEs under the dry-coupling and wet-coupling regimes, respectively, we present three statistical measures of APEs as a function of B_{LT} in Figure 6. Figure 6a shows that, for the dry-coupling cases, the fractional occurrence of APEs (defined as the proportion of APEs relative to all dry-coupling cases) in each B_{LT} bin increases with B_{LT} up to its 70th percentile, with a significant correlation ($R = 0.65$, $p < 0.05$). For the wet-coupling cases, the fractional occurrence of the APEs peaks when B_{LT} is between the
255 30th and 70th percentile. Thus, APEs appear to prefer higher LT humidity under dry coupling than under wet coupling. Next, we explore how B_{LT} affects the partition of dry-coupling versus wet-coupling APEs. Figure 6b shows that the proportion of the dry-coupling APEs relative to all APEs increases with B_{LT} , with a strong correlation ($R = 0.89$, $p < 0.05$). The proportion ranges from 0.04 at the bottom 10% to 0.47 at the top 10% of B_{LT} . However, the proportion of wet-coupling APEs per B_{LT} bin peaks at lower to medium B_{LT} percentiles (30%-50%) and decreases almost
260 monotonically with increasing B_{LT} from 50% to 100%.

We also investigate how B_{LT} affects rain rates associated with dry-coupling and wet-coupling APEs, respectively. Figure 6c shows a clear increase in rain rate with B_{LT} for the dry-coupling APEs, except for the 90-100th percentile of B_{LT} , where there are few APEs samples. In contrast, we find no clear dependence of rain rate on B_{LT} for the wet-coupling APEs. Thus, our findings suggest that a high B_{LT} tends to increase the frequency and intensity of the dry-coupling APEs, as well as the relative frequency of dry-coupling APEs compared to wet-coupling APEs.
265

In addition, we evaluate the variations of deep- (cloud top height (CTH) > 8 km), shallow- (CTH < 3 km), and convective congestus (CTH between 3 km and 8 km) associated with APEs based on hourly precipitation and cloud fraction as in Zhuang et al. (2017, Figure S2). In general, APEs associated with all three convective types increase with B_{LT} under dry-coupling conditions. Under wet-coupling condition, APEs associated with deep convection does not exhibit a clear dependence on B_{LT} . However, APEs associated with shallow convection decreases with increasing
270 B_{LT} , while those associated with congestus increase with increasing B_{LT} . These results imply that the increase in B_{LT} can lead to a deepening of shallow convection into congestus due to reduced buoyancy dilution caused by entraining wetter LT air for wet-coupling convection.

4 Conclusions

275 Land-atmosphere interactions occur when local land surface and subsurface conditions influence the moisture and energy budgets of the overlying atmosphere. The relative impacts of soil moisture on convective precipitation can



vary depending on the atmospheric conditions. In this study, we compared the difference in RH, q , and T profiles between APEs and non-APEs under both dry- and wet-coupling conditions.

Our initial analysis revealed that APEs had an overall wetter PBL and LT (0-4km AGL) than non-APEs, especially under dry-coupling regimes. The RH difference between APEs and non-APEs in the LT was driven by differences in both q and T , with dry-coupling APEs exhibiting lower humidity in the PBL than wet-coupling APEs. However, as the altitude increases, the difference in RH between dry- and wet-coupling APEs decreases due to the increasing difference in q and decreasing difference in T . Above 4 km AGL, the difference in q becomes zero. Therefore, we could infer the importance of LT humidity in the SM-P relationship, and the APEs under dry-coupling conditions necessitate more LT humidity than that under wet-coupling conditions.

To further investigate the influence of LT humidity on the SM-P relationship, we employ an entraining parcel model and a new metric B_{LT} , which measures the 2-4 km vertical integral of the difference between buoyancy calculated from the observed humidity profile and that correlated to (regressed against) the average specific humidity in the PBL. Statistical analysis reveals that the wetter LT and normal PBL were associated with larger B_{LT} values, whereas drier LT was linked to smaller B_{LT} values. Moreover, there is a higher likelihood of APEs occurring with positive B_{LT} percentile under dry-coupling conditions, while this relationship is not apparent for the probability distribution of B_{LT} percentile for wet-coupling APEs. Additionally, as the B_{LT} percentile increases, the frequency of dry-coupling APEs also increases, whereas the opposite tendency was observed for wet-coupling APEs. In the meantime, the ratio of dry-coupling APEs to all APEs increases with the B_{LT} percentile, while this tendency is the opposite for the ratio of wet-coupling APEs to all APEs. Regarding precipitation, the average rain rate tends to rise with increasing B_{LT} percentile under dry-coupling conditions, but this trend is not significant for wet-coupling APEs. Overall, our results indicate that the impact of LT humidity differs between dry- and wet-coupling APEs, with dry-coupling APEs being more influenced by LT humidity compared to wet-coupling APEs.

The Great Plain Low-Level Jet (GPLLJ) is widely acknowledged as a primary mechanism responsible for the regional-scale water vapor transport from the Gulf of Mexico during May-September. The GPLLJ creates a thermodynamic environment that facilitates convection and precipitation, making it a key factor in initiating and sustaining mesoscale weather phenomena (e.g., Higgins et al., 1997; Hodges & Pu, 2019; Mo et al., 1997; Pu et al., 2016; Pu & Dickinson, 2014; Weaver & Nigam, 2008). It is well established that the GPLLJ can enhance the occurrence of nocturnal convective precipitation in the SGP (Pu and Dickinson, 2014). However, our findings imply that the moisture carried by the GPLLJ could also play an important role in generating local diurnal afternoon precipitation when it reaches the region during the daytime, particularly over dry soil conditions. This result is consistent with Ford et al. (2015) that suggested soil moisture feedback to precipitation could potentially manifest itself over wetter- and drier-than-normal soils, depending on the overall synoptic and dynamic conditions, and precipitation favors dry soil when the low-level jet is present. Therefore, these results collectively suggest that the GPLLJ plays a significant role in alleviating drought conditions in the SGP by influencing both diurnal and nocturnal precipitation.

This work reveals the varying impact of LT humidity on the SM-P relationship, highlighting the importance of incorporating land-atmosphere interaction into model parameterizations. Our future work will involve investigating the primary source of LT humidity and employing both B_{LT} and CTP/HI_{Low} as an atmospheric indicator to identify the



315 global region exhibiting various LT humidity-SM-P relationship, advancing our knowledge of LAC on a broader scale.

Competing Interests

The contact author has declared that none of the authors has any competing interests.

Acknowledgment

320 G.W. was funded by the China Scholarship Council (CSC; 201806010052). Y.Z. and R.F. were supported by the National Oceanic and Atmospheric Administration-Climate Program Office (NOAA-CPO) Modelling, Analysis, Predictions, and Projections (MAPP) Program (NA20OAR4310426), and the National Science Foundation (NSF) Physical and Dynamic Meteorology (PDM) Program (AGS-2214697).

Reference

- 325 Bretherton, C. S., Peters, M. E., and Back, L. E.: Relationships between water vapor path and precipitation over the tropical oceans, *J Clim*, [https://doi.org/10.1175/1520-0442\(2004\)017<1517:RBWVPA>2.0.CO;2](https://doi.org/10.1175/1520-0442(2004)017<1517:RBWVPA>2.0.CO;2), 2004.
- Ek, M. B. and Holtslag, A. A. M.: Influence of soil moisture on boundary layer cloud development, *J Hydrometeorol*, 5, 86–99, [https://doi.org/10.1175/1525-7541\(2004\)005<0086:IOSMOB>2.0.CO;2](https://doi.org/10.1175/1525-7541(2004)005<0086:IOSMOB>2.0.CO;2), 2004.
- Ferguson, C. R. and Wood, E. F.: An evaluation of satellite remote sensing data products for land surface hydrology: Atmospheric infrared sounder, *J Hydrometeorol*, 11, 1234–1262, <https://doi.org/10.1175/2010JHM1217.1>, 2010.
- 330 Fernando, D. N., Mo, K. C., Fu, R., Pu, B., Bowerman, A., Scanlon, B. R., Solis, R. S., Yin, L., Mace, R. E., Mioduszewski, J. R., Ren, T., and Zhang, K.: What caused the spring intensification and winter demise of the 2011 drought over Texas?, *Clim Dyn*, 47, 3077–3090, <https://doi.org/10.1007/s00382-016-3014-x>, 2016.
- Findell, K. L. and Eltahir, E. A. B.: Atmospheric controls on soil moisture-boundary layer interactions. Part I: Framework development, *J Hydrometeorol*, 4, 552–569, [https://doi.org/10.1175/1525-7541\(2003\)004<0552:ACOSML>2.0.CO;2](https://doi.org/10.1175/1525-7541(2003)004<0552:ACOSML>2.0.CO;2), 2003.
- 335 Ford, T. W., Rapp, A. D., and Quiring, S. M.: Does afternoon precipitation occur preferentially over dry or wet soils in Oklahoma?, *J Hydrometeorol*, <https://doi.org/10.1175/JHM-D-14-0005.1>, 2015.
- Fulton, R. A., Breidenbach, J. P., Seo, D. J., Miller, D. A., and O'Bannon, T.: The WSR-88D rainfall algorithm, *Weather Forecast*, [https://doi.org/10.1175/1520-0434\(1998\)013<0377:TWRA>2.0.CO;2](https://doi.org/10.1175/1520-0434(1998)013<0377:TWRA>2.0.CO;2), 1998.
- 340 Gentine, P., Holtslag, A. A. M., D'Andrea, F., and Ek, M.: Surface and atmospheric controls on the onset of moist convection over land, *J Hydrometeorol*, 14, 1443–1462, <https://doi.org/10.1175/JHM-D-12-0137.1>, 2013.
- Guo, Z., Dirmeyer, P. A., Koster, R. D., Bonan, G., Chan, E., Cox, P., Gordon, C. T., Kanae, S., Kowalczyk, E., Lawrence, D., Liu, P., Lu, C. H., Malyshev, S., McAvaney, B., McGregor, J. L., Mitchell, K., Mocko, D., Oki, T., Oleson, K. W., Pitman, A., Sud, Y. C., Taylor, C. M., Verseghy, D., Vasic, R., Xue, Y., and Yamada, T.: GLACE:



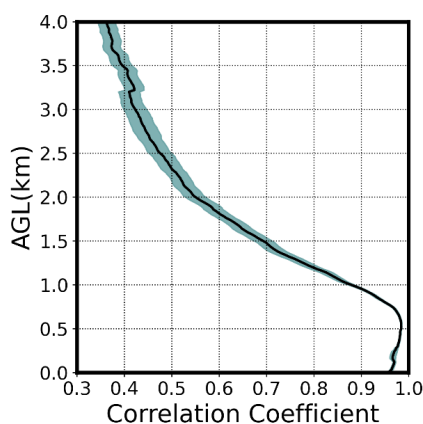
- 345 The Global Land-Atmosphere Coupling Experiment. Part II: Analysis, *J Hydrometeorol*, 7, 611–625,
<https://doi.org/10.1175/JHM511.1>, 2006.
- Higgins, R. W., Yao, Y., Yarosh, E. S., Janowiak, J. E., and Mo, K. C.: Influence of the Great Plains Low-Level Jet
on Summertime Precipitation and Moisture Transport over the Central United States, *Journal of Climate*, American
Meteorological Society, 481–507 pp., [https://doi.org/10.1175/1520-0442\(1997\)010<0481:IOTGPL>2.0.CO;2](https://doi.org/10.1175/1520-0442(1997)010<0481:IOTGPL>2.0.CO;2), 1997.
- 350 Hodges, D. and Pu, Z.: Characteristics and variations of low-level jets in the contrasting warm season precipitation
extremes of 2006 and 2007 over the Southern Great Plains, *Theor Appl Climatol*, 136, 753–771,
<https://doi.org/10.1007/S00704-018-2492-7/FIGURES/19>, 2019.
- Holloway, C. E. and Neelin, D. J.: Moisture vertical structure, column water vapor, and tropical deep convection, *J*
Atmos Sci, 66, 1665–1683, <https://doi.org/10.1175/2008JAS2806.1>, 2009.
- 355 Huang, H. Y. and Margulis, S. A.: Investigating the impact of soil moisture and atmospheric stability on cloud
development and distribution using a coupled large-eddy simulation and land surface model, *J Hydrometeorol*,
<https://doi.org/10.1175/2011JHM1315.1>, 2011.
- Illston, B. G., Basara, J. B., Fisher, D. K., Elliott, R., Fiebrich, C. A., Crawford, K. C., Humes, K., and Hunt, E.:
Mesoscale monitoring of soil moisture across a statewide network, *J Atmos Ocean Technol*,
360 <https://doi.org/10.1175/2007JTECHA993.1>, 2008.
- Konings, A. G., Katul, G. G., and Porporato, A.: The rainfall-no rainfall transition in a coupled land-convective
atmosphere system, *Geophys Res Lett*, <https://doi.org/10.1029/2010GL043967>, 2010.
- Koster, R. D., Guo, Z., Dirmeyer, P. A., Bonan, G., Chan, E., Cox, P., Davies, H., Gordon, C. T., Kanae, S.,
Kowalczyk, E., Lawrence, D., Liu, P., Lu, C. H., Malyshev, S., McAvaney, B., Mitchell, K., Mocko, D., Oki, T.,
365 Oleson, K. W., Pitman, A., Sud, Y. C., Taylor, C. M., Verseghy, D., Vasic, R., Xue, Y., and Yamada, T.: GLACE:
The Global Land-Atmosphere Coupling Experiment. Part I: Overview, <https://doi.org/10.1175/JHM510.1>, 2006.
- Liu, S. and Liang, X. Z.: Observed diurnal cycle climatology of planetary boundary layer height, *J Clim*,
<https://doi.org/10.1175/2010JCLI3552.1>, 2010.
- Mapes, B., Tulich, S., Lin, J., and Zuidema, P.: The mesoscale convection life cycle: Building block or prototype for
370 large-scale tropical waves?, *Dynamics of Atmospheres and Oceans*, <https://doi.org/10.1016/j.dynatmoce.2006.03.003>,
2006.
- Mo, K. C., Paegle, J. N., and Higgins, R. W.: Atmospheric processes associated with summer floods and droughts in
the central United States, *J Clim*, [https://doi.org/10.1175/1520-0442\(1997\)010<3028:APAWSF>2.0.CO;2](https://doi.org/10.1175/1520-0442(1997)010<3028:APAWSF>2.0.CO;2), 1997.
- Myoung, B. and Nielsen-Gammon, J. W.: The convective instability pathway to warm season drought in Texas. Part
375 I: The role of convective inhibition and its modulation by soil moisture, *J Clim*,
<https://doi.org/10.1175/2010JCLI2946.1>, 2010.
- Pu, B. and Dickinson, R. E.: Diurnal Spatial Variability of Great Plains Summer Precipitation Related to the Dynamics
of the Low-Level Jet, *J Atmos Sci*, 71, 1807–1817, <https://doi.org/10.1175/JAS-D-13-0243.1>, 2014.
- Pu, B., Dickinson, R. E., and Fu, R.: Dynamical connection between Great Plains low-level winds and variability of
380 central Gulf States precipitation, *Journal of Geophysical Research: Atmospheres*, 121, 3421–3434,
<https://doi.org/10.1002/2015JD024045>, 2016.



- Raz-Yaseef, N., Billesbach, D. P., Fischer, M. L., Biraud, S. C., Gunter, S. A., Bradford, J. A., and Torn, M. S.: Vulnerability of crops and native grasses to summer drying in the U.S. Southern Great Plains, *Agric Ecosyst Environ*, <https://doi.org/10.1016/j.agee.2015.07.021>, 2015.
- 385 Roundy, J. K. and Santanello, J. A.: Utility of Satellite Remote Sensing for Land–Atmosphere Coupling and Drought Metrics, *J Hydrometeorol*, 18, 863–877, <https://doi.org/10.1175/jhm-d-16-0171.1>, 2017.
- Roundy, J. K., Ferguson, C. R., and Wood, E. F.: Temporal Variability of Land-Atmosphere Coupling and Its Implications for Drought over the Southeast United States, *J Hydrometeorol*, 14, 622–635, <https://doi.org/10.1175/JHM-D-12-090.1>, 2013.
- 390 Santanello, J. A., And, J. R., Peters-Lidard, C. D., Kumar, S. v, Alonge, C., and Tao, W.-K.: A Modeling and Observational Framework for Diagnosing Local Land-Atmosphere Coupling on Diurnal Time Scales, *J. Hydrometeorol*, 10, 577–599, <https://doi.org/10.1175/2009JHM1066.1>, 2009.
- Santanello, J. A., Dirmeyer, P. A., Ferguson, C. R., Findell, K. L., Tawfik, A. B., Berg, A., Ek, M., Gentine, P., Guillod, B. P., van Heerwaarden, C., and Roundy, J.: LAND-ATMOSPHERE INTERACTIONS The LoCo
395 Perspective, <https://doi.org/10.1175/BAMS-D-17-0001.1>, 2017.
- Santanello, J. A., Dirmeyer, P. A., Ferguson, C. R., Findell, K. L., Tawfik, A. B., Berg, A., Ek, M., Gentine, P., Guillod, B. P., Van Heerwaarden, C., Roundy, J., and Wulfmeyer, V.: Land–Atmosphere Interactions: The LoCo Perspective, *Bull Am Meteorol Soc*, 99, 1253–1272, <https://doi.org/10.1175/BAMS-D-17-0001.1>, 2018.
- Schiro, K. A., Neelin, J. D., Adams, D. K., and Lintner, B. R.: Deep convection and column water vapor over tropical
400 land versus tropical ocean: A comparison between the amazon and the tropical Western Pacific, *J Atmos Sci*, 73, 4043–4063, <https://doi.org/10.1175/JAS-D-16-0119.1>, 2016.
- Schiro, K. A., Ahmed, F., Giangrande, S. E., and David Neelin, J.: GoAmazon2014/5 campaign points to deep-inflow approach to deep convection across scales, 115, 4577–4582, <https://doi.org/10.1073/pnas.1719842115>, 2018.
- Schneider, J. M., Flsher, D. K., Elliott, R. L., Brown, G. O., and Bahrman, C. P.: Spatiotemporal variations in soil
405 water: First results from the ARM SGP CART network, *J Hydrometeorol*, [https://doi.org/10.1175/1525-7541\(2003\)004<0106:SVISWF>2.0.CO;2](https://doi.org/10.1175/1525-7541(2003)004<0106:SVISWF>2.0.CO;2), 2003.
- Seneviratne, S. I., Corti, T., Davin, E. L., Hirschi, M., Jaeger, E. B., Lehner, I., Orlowsky, B., and Teuling, A. J.: Investigating soil moisture–climate interactions in a changing climate: A review, *Earth Sci Rev*, 99, 125–161, <https://doi.org/10.1016/j.earscirev.2010.02.004>, 2010.
- 410 Siebesma, A. P., Soares, P. M. M., and Teixeira, J.: A Combined Eddy-Diffusivity Mass-Flux Approach for the Convective Boundary Layer, <https://doi.org/10.1175/JAS3888.1>, 2007.
- Song, H. J., Ferguson, C. R., and Roundy, J. K.: Land-atmosphere coupling at the southern great plains atmospheric radiation measurement (ARM) field site and its role in anomalous afternoon peak precipitation, *J Hydrometeorol*, 17, 541–556, <https://doi.org/10.1175/JHM-D-15-0045.1>, 2016.
- 415 Tawfik, A. B., Dirmeyer, P. A., and Santanello, J. A.: The heated condensation framework. Part I: Description and southern great plains case study, *J Hydrometeorol*, 16, 1929–1945, <https://doi.org/10.1175/JHM-D-14-0117.1>, 2015a.



- Tawfik, A. B., Dirmeyer, P. A., and Santanello, J. A.: The heated condensation framework. Part II: Climatological behavior of convective initiation and land-atmosphere coupling over the conterminous United States, *J Hydrometeorol*, 16, 1946–1961, <https://doi.org/10.1175/JHM-D-14-0118.1>, 2015b.
- 420 Taylor, C. M.: Detecting soil moisture impacts on convective initiation in Europe, *Geophys Res Lett*, 42, 4631–4638, <https://doi.org/10.1002/2015GL064030>, 2015.
- Tuttle, S. and Salvucci, G.: Atmospheric science: Empirical evidence of contrasting soil moisture-precipitation feedbacks across the United States, *Science* (1979), 352, 825–828, <https://doi.org/10.1126/science.aaa7185>, 2016.
- Wakefield, R. A., Basara, J. B., Furtado, J. C., Illston, B. G., Ferguson, C. R., and Klein, P. M.: A modified framework for quantifying land–atmosphere covariability during hydrometeorological and soil wetness extremes in oklahoma, *J Appl Meteorol Climatol*, 58, 1465–1483, <https://doi.org/10.1175/JAMC-D-18-0230.1>, 2019.
- 425 Weaver, S. J. and Nigam, S.: Variability of the Great Plains Low-Level Jet: Large-Scale Circulation Context and Hydroclimate Impacts, *J Clim*, 21, 1532–1551, <https://doi.org/10.1175/2007JCLI1586.1>, 2008.
- Wilks, D. S.: *Statistical methods in the atmospheric sciences*, 676, 2011.
- 430 Yin, J., Albertson, J. D., Rigby, J. R., and Porporato, A.: Land and atmospheric controls on initiation and intensity of moist convection: CAPE dynamics and LCL crossings, *Water Resour Res*, 51, 8476–8493, <https://doi.org/10.1002/2015WR017286>, 2015.
- Zhang, Y. and Klein, S. A.: Mechanisms Affecting the Transition from Shallow to Deep Convection over Land: Inferences from Observations of the Diurnal Cycle Collected at the ARM Southern Great Plains Site, *J Atmos Sci*, 67, 2943–2959, <https://doi.org/10.1175/2010jas3366.1>, 2010.
- 435 Zhuang, Y., Fu, R., Marengo, J. A., and Wang, H.: Seasonal variation of shallow-to-deep convection transition and its link to the environmental conditions over the Central Amazon, *J Geophys Res*, 122, 2649–2666, <https://doi.org/10.1002/2016JD025993>, 2017.
- Zhuang, Y., Fu, R., and Wang, H.: How do environmental conditions influence vertical buoyancy structure and shallow-to-deep convection transition across different climate regimes?, *J Atmos Sci*, 75, 1909–1932, <https://doi.org/10.1175/JAS-D-17-0284.1>, 2018.
- 440





445 **Figure 1: Correlation coefficient profiles between specific humidity (q) at each vertical level from 0 to 4 km AGL and mean q in the mixed layer (0-1km AGL). The correlation coefficients are calculated for the warm season of each year. The black line indicates the average value of 18 years, and the green shade shows the standard error.**

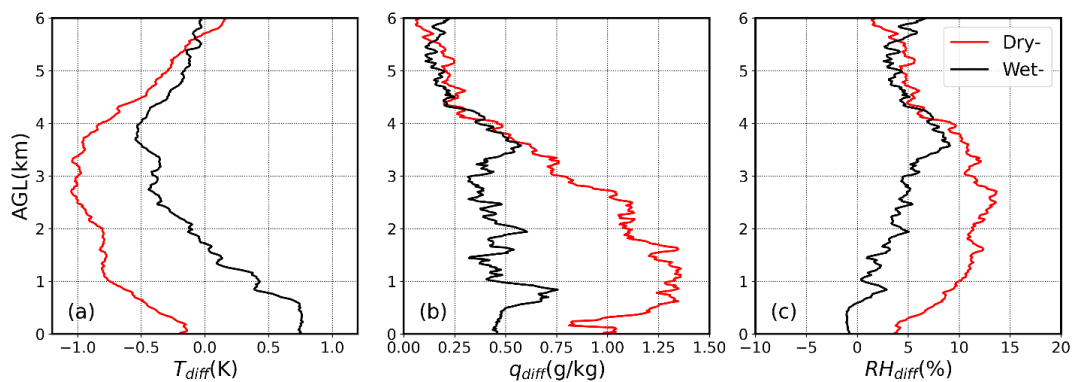
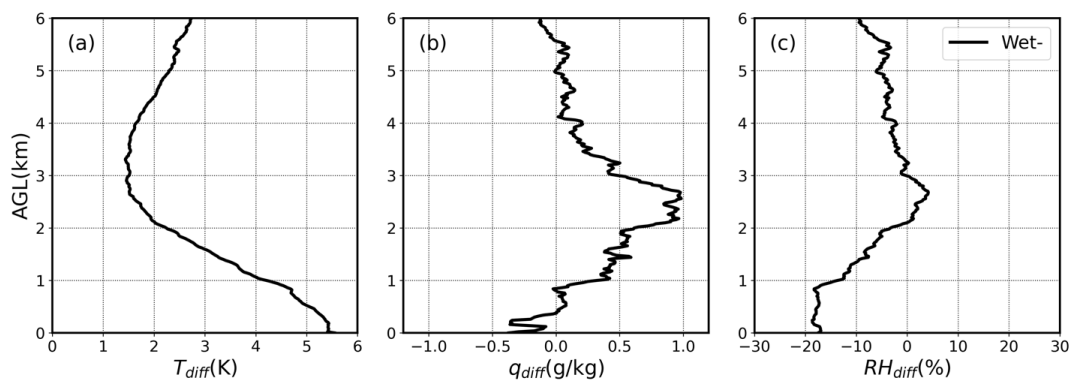
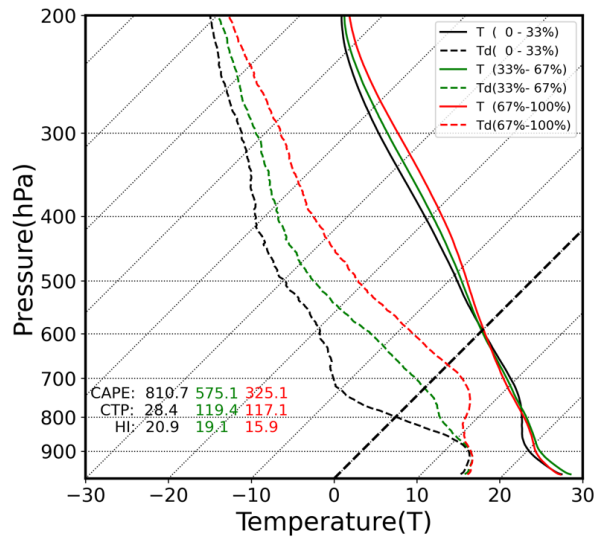


Figure 2: Composite difference of a) temperature (T_{diff}), b) specific humidity (q_{diff}), and c) relative humidity (RH_{diff}) profiles between APEs and non-APEs for dry- (red lines) and wet- (black lines) coupling cases.



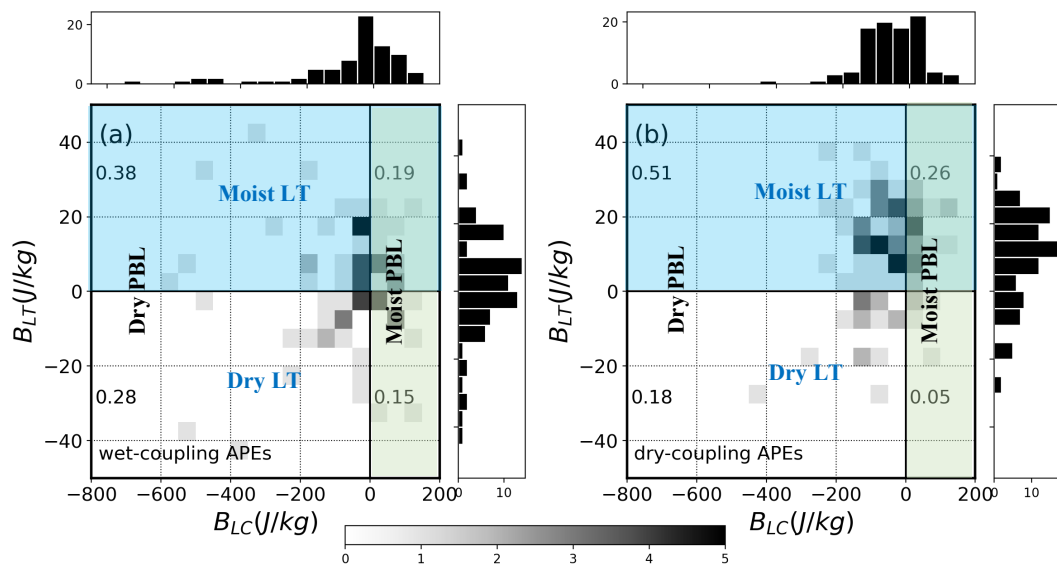
450

Figure 3: Composite difference of a) temperature (T_{diff}), b) specific humidity (q_{diff}), and c) relative humidity (RH_{diff}) between dry- and wet-coupling APEs (Dry minus Wet).



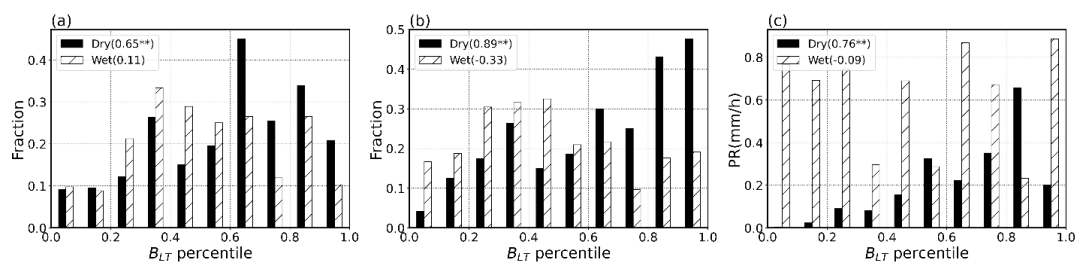
455

Figure 4: Composite temperature (T ; solid line) and dewpoint temperature (T_d ; dash line) profiles at the ARM SGP site for all days during May–September from 2001 to 2018, above the 950hPa level, based on B_{LT} tercile: 0-33% (lower B_{LT} , black); 33%-67% (medium B_{LT} , green); 67%-100% bins (higher B_{LT} , red).



460

Figure 5: Joint frequency distributions of a) wet-coupling APEs and b) dry-coupling APEs as a function of B_{LT} (representing contribution of LT humidity to convective buoyancy) and B_{LC} (representing contribution of surface humidity) with white shades representing no APEs and darkest shades representing more than 5 APEs occurs of each $B_{LC} - B_{LT}$ bin. The number indicates the fraction in each quadrant.



465 **Figure 6:** (a) The fraction of wet- (dry-) coupling APEs over wet- (dry-) coupling cases ($\frac{N_{wet-coupling-APEs}}{N_{wet-coupling-cases}}$ or $\frac{N_{dry-coupling-APEs}}{N_{dry-coupling-cases}}$)
 in each B_{LT} bin for the dry- and wet-coupling cases, respectively. (b) Same as (a), but for the percentage of wet- or dry-
 470 coupling APEs relative to all APEs ($\frac{N_{wet-coupling-APEs}}{N_{APEs}}$ and $\frac{N_{dry-coupling-APEs}}{N_{APEs}}$). (c) Same as (a), but for the mean afternoon
 precipitation rate (PR). The correlation coefficients between B_{LT} percentiles and the fraction/PR are listed for the dry- and
 wet-coupling cases, respectively; correlation coefficients between B_{LT} percentiles and y-axis value significant at 0.05 level
 are marked with two asterisks.